Author(s): Vinnurva, J. & Alava, M. & Ala-Nissilä, Tapio & Krug, J.

Title: Kinetic roughening in fiber deposition

Year: 1998

Version: Final published version

Please cite the original version:

Vinnurva, J. & Alava, M. & Ala-Nissilä, Tapio & Krug, J. 1998. Kinetic roughening in fiber deposition. Physical Review E. Volume 58, Issue 1. P. 1125-1131. ISSN 1539-3755 (printed). DOI: 10.1103/physreve.58.1125.

Kinetic roughening in fiber deposition

J. Vinnurva,[1,3] M. Alava,[1,2] T. Ala-Nissila,[3,4,*] and J. Krug[5]
[1]*Laboratory of Physics, Helsinki University of Technology, P.O. Box 1100, FIN-02015 HUT, Finland*
[2]*NORDITA, Blegdamsvej 17, DK-2100 Copenhagen, Denmark*
[3]*Helsinki Institute of Physics, University of Helsinki, P.O. Box 9 (Siltavuorenpenger 20 C), FIN-00014, Helsinki, Finland*
[4]*Department of Physics, Brown University, Box 1843, Providence, Rhode Island 02912*
[5]*Fachbereich Physik, Universität Gesamthochschule Essen, D-45117 Essen, Germany*
(Received 7 November 1997)

We consider the kinetic roughening of growing interfaces in a simple model of fiber deposition [K. J. Niskanen and M. J. Alava, Phys. Rev. Lett. **73**, 3475 (1994)]. Fibers of length L_f are deposited randomly on a lattice and upon deposition allowed to bend down locally by a distance determined by the flexibility parameter T_f. For $T_f<\infty$ overhangs are allowed and pores develop in the bulk of the deposit, which leads to kinetic roughening of the growing surface. We have numerically determined the asymptotic scaling exponents for a one-dimensional version of the model and find that they are compatible with the Kardar-Parisi-Zhang equation. We study in detail the dependence of the tilt-dependent growth velocity on T_f and develop analytic arguments to explain the simulation results in the limit of small and large tilts. [S1063-651X(98)04906-X]

PACS number(s): 02.70.−c, 68.55.Jk, 64.60.Ht, 05.40.+j

I. INTRODUCTION

Nonequilibrium properties of driven interfaces have attracted considerable interest recently due to theoretical reasons and the importance of growth processes on surfaces under molecular beam epitaxy conditions [1,2]. From the theoretical point of view, a particularly important property of driven interfaces is the ability to classify the growth dynamics according to the forms of the underlying stochastic differential equations that describe different physical systems. The simplest nonlinear growth equation of this type is the celebrated Kardar-Parisi-Zhang (KPZ) equation [3]

$$\frac{\partial h(\vec{r},t)}{\partial t}=\nabla^2 h(\vec{r},t)+\frac{\lambda}{2}|\nabla h(\vec{r},t)|^2+\eta(\vec{r},t)+v_0, \quad (1)$$

where $h(\vec{r},t)$ is a single-valued height variable, $\eta(\vec{r},t)$ is a Gaussian (white) noise term, and v_0 is a constant. The crucial ingredient in the KPZ equation is the nonlinear term proportional to λ, which manifests itself in the nontrivial tilt dependence of the velocity of the growing interface. One of the physically most interesting quantities associated with interface roughening is the average width, i.e., the standard deviation of $h(\vec{r},t)$, which becomes a function of time and the system size L:

$$w^2(L,t)=\overline{\langle[h(\vec{r},t)-\overline{h}(t)]^2\rangle}, \quad (2)$$

where $\overline{h}(t)$ denotes the spatial average of $h(\vec{r},t)$ and the angular brackets denote an average over the noise. The width scales according to the Family-Vicsek scaling relation [4] as

$$w(L,t)=L^{\chi}f(t/L^z), \quad (3)$$

where the scaling function $f(y)$ behaves as

$$f(y)\sim\begin{cases} y^{\beta} & \text{for } y\ll 1 \\ \text{const} & \text{for } y\gg 1. \end{cases} \quad (4)$$

The dynamical exponent z, the roughness exponent χ, and the growth exponent β are linked by $\chi=z\beta$ and the scaling relation $\chi+z=2$. For a one-dimensional (1D) interface, the stationary probability distribution associated with Eq. (1) is known and the exponents are given by $\beta=1/3$, $\chi=1/2$, and $z=3/2$.

Perhaps the easiest way to study the properties of the KPZ universality class is through simple lattice deposition models of interface growth, many of which are described asymptotically by Eq. (1). In some cases, the connection between such models and the KPZ equation can be made explicit and the parameter λ calculated analytically [2]. Experimentally, however, the KPZ universality class has proved to be elusive, with the strongest evidence to date coming from slow combustion experiments of paper sheets [5].

In this paper we address the surface roughening of planar fiber networks, which is an interesting candidate for kinetic roughening. We employ a model for random deposition of flexible fibers on a lattice [6,7], which was originally introduced to describe the bulk properties of 3D random fiber networks, the prime example being ordinary paper. The bulk structures obtained from the model seem to describe well, e.g., the pore geometry of random fiber assemblies measured by creeping flow permeability [8] or light scattering properties of paper [9].

For surface roughening, the essential parameters in the model are the fiber length L_f in lattice units and the flexibility T_f of the deposited fibers, which induces overhangs in the bulk that constitute the eventual pore structure. It is known through studies of surface growth models that such bulk defects play an important role in the kinetic roughening of growing surfaces [2,10]. Thus it is of interest to study how this occurs in the case of fiber deposition as well.

*Author to whom correspondence should be addressed. Electronic address: alanissi@csc.fi

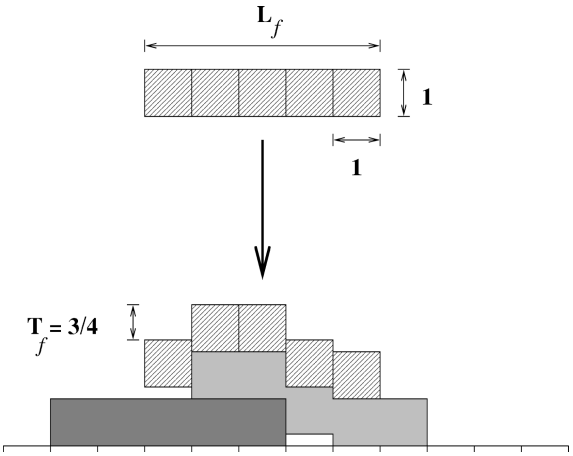

FIG. 1. Deposition of a fiber with length $L_f=5$ and flexibility $T_f=3/4$.

One should note that the model does not reproduce the surface roughness properties of real paper sheets [11]. This is due to several simplifying assumptions. In the case of real paper, hydrodynamics is expected to play an important role. There are indeed nontrivial mass correlations [12] and clustering of fibers [13] present that have their origin in hydrodynamics during formation, similarly to the sedimentation problem [14,15]. Another factor missing from simple deposition models is due to the details of the paper manufacturing process. For instance, ordinary paper sheets are usually compressed mechanically. Such effects are hard to take into account as they depend on the actual initial spatial structure of the deposit itself [16].

In this paper our aim is to present a detailed study of the surface growth properties of the fiber deposition model described above and study the dependence of growth on the relevant parameters. Here we concentrate on the growth of 1D interfaces for simplicity. We start by briefly describing the deposition model in Sec. II. In Sec. III we present results of extensive numerical simulations of the kinetic roughening in the model. As expected, for any finite value of the flexibility parameter T_f, the kinetic roughening in the model is asymptotically described by the KPZ equation. We discuss in detail growth on tilted surfaces in the limits of small and large tilts and present analytic arguments for the scaling behavior of the parameter λ in the KPZ equation. Finally, Sec. IV contains our conclusions and a discussion.

II. MODEL

In the model, fibers of length L_f are deposited on a flat substrate of size L with periodic boundary conditions. The original model is two dimensional, while here we will discuss the 1D version only. The ''fibers'' in the model are discretized to squares of size one in lattice units and form a chain of length L_f (see Fig. 1). The flexibility of the fibers T_f is defined to be the maximum vertical displacement allowed between two neighboring squares in a fiber in units of fiber thickness. Thus the larger T_f is, the more flexible the fibers are. The limit $T_f=0$ refers to completely stiff fibers.

The fibers are deposited one by one randomly onto the lattice. During deposition they are kept straight and parallel to the substrate. The part (or parts) of a fiber that first touches the underlying network stops moving and the rest of the fiber bends further down until either all parts touch the network beneath them or the maximum bending allowed by the deflection constraint T_f is reached. Note that this rule conserves just the projection of the fiber on the lattice, but due to the allowed vertical displacements the fiber may stretch. Time is defined in terms of coverage, which is the amount of mass deposited per unit substrate length. Since the mass of a fiber is L_f, the deposition of N fibers on a lattice of size L takes $t=N(L_f/L)$ time steps.

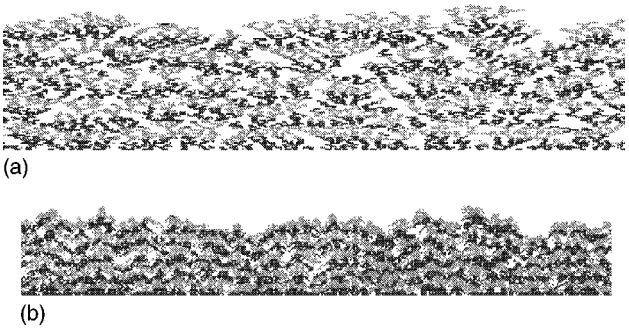

FIG. 2. Typical fiber networks with (a) $T_f=0.1$ and (b) $T_f=1.0$. The system size $L=500$ and the fiber length $L_f=5$. The white areas are pores and the gray areas indicate the fibers. The number of fibers is 5000 and each layer marked by either of the two shades of gray contains 500 fibers.

The resulting network has different top and bottom surfaces because the fibers at the bottom are generally less deformed than the fibers at the top due to the closeness of the substrate. Here we examine only the behavior of the free top surface. It is defined by the set of local height variables $h(x,t)$ at each lattice site x. Thus the curve defined by $h(x,t)$ is a single-valued function so that overhangs in the surface structure are ignored. If the number of particles deposited in a unit time is kept constant, the spatial average of the surface height $\overline{h}(t)\equiv\Sigma_{i=1}^{L}h(x_i,t)/L$ grows linearly in time.

Starting from a flat surface, the roughness of the emerging top surface develops in time in a way that clearly depends on T_f. The parameter T_f controls the porosity of the network: high values of T_f give a more dense network and low values a more porous one, as can be seen from Fig. 2.

III. RESULTS

A. Scaling exponents

To determine the scaling exponents associated with surface growth, we computed the surface width $w(L,t)$ for four different system sizes ($L=1000$, 1500, 2500, and 5000) with the fiber flexibilities $T_f=0.1$ and 1.0 and with various fiber lengths. The results shown here are for $T_f=1.0$ and $L_f=5$. At very early times, there is a regime where the fibers are uncorrelated corresponding to the random deposition (RD) case [1] (see the discussion at the end of this section). Following this, the data can be fitted to the form

$$w(L,t)=a(L)t^{\beta}, \tag{5}$$

where $a(L)$ is a function of L. The error estimate was obtained by calculating the difference between the maximum

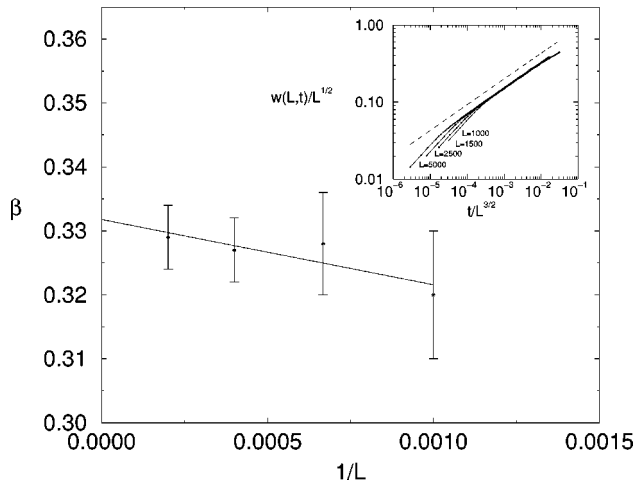

FIG. 3. β as a function of $1/L$ for $T_f=1.0$ and $L_f=5$. The solid line is a least-squares fit to the four data points. Extrapolation as $L\to\infty$ gives $\beta=0.33\pm0.01$. The inset shows the scaling function $f(t/L^z)$ and the dashed line has a slope of 1/3.

value of β with which the curve (5) still remains within the error bars of the data points (which were calculated from the standard deviation of the data) and the growth exponent given by a standard least-squares fit.

Figure 3 shows β as a function of $1/L$ as obtained from the data for $w(L,t)$. An extrapolation from the four data points to $L\to\infty$ gives $\beta=0.33\pm0.01$. In the inset, we also show the scaling function $f(t/L^z)$ for a variety of system sizes.

We also checked the consistency of the results by eliminating any additive constants from $w(L,t)$ through [17]

$$\tilde{w}(L,t)\equiv w(L,2t)-w(L,t). \tag{6}$$

Although this method gave slightly lower values for β than the direct application of the least-squares method, a similar extrapolation procedure as above gave again $\beta=0.33\pm0.01$ as $L\to\infty$ for $T_f=1.0$ and $L_f=5$. Thus we take this to be our best estimate for β.

Another way to determine the scaling exponents for a given system is to study various height-height correlation functions [1,17]. The general two-point correlation function is defined as

$$C_g(r,t,t')\equiv\langle\overline{[\delta h(x+r,t+t')-\delta h(x,t)]^2}\rangle, \tag{7}$$

where $\delta h(x,t)\equiv h(x,t)-\overline{h}(t)$. The equal-time height-height correlation function can now be defined as

$$G_h(r,t)\equiv C_g(r,t,t'=0), \tag{8}$$

which asymptotically behaves as

$$G_h(r,t)\sim\begin{cases} r^{2\chi} & \text{for } r\ll t^{1/z} \\ t^{2\beta} & \text{for } r\gg t^{1/z}. \end{cases} \tag{9}$$

Averaging $G_h(r,t)$ over r for $r\gg t^{1/z}$, only the short-wavelength components are lost and the corresponding function $\hat{G}_h(t)$ behaves as

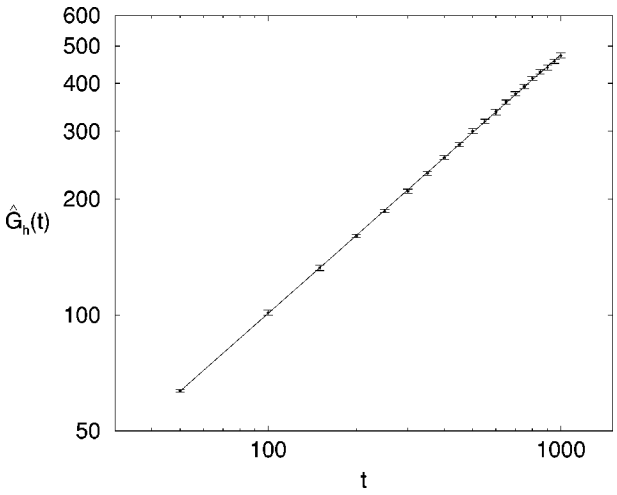

FIG. 4. $\hat{G}_h(t)$ for a system with $L=5000$, $T_f=1.0$, and $L_f=5$ on a log-log scale. A direct application of the least-squares fitting method gives $\beta=0.338\pm0.003$. The error bars are calculated from the standard deviation of $\hat{G}_h(t)$.

$$\hat{G}_h(t)\sim t^{2\beta}. \tag{10}$$

We calculated the equal-time height-height correlation function of Eq. (8) for a system with $L=5000$, $T_f=1.0$, and $L_f=5$. Figure 4 shows the corresponding $\hat{G}_h(t)$ on a log-log scale. The error bars indicate the standard deviation of $\hat{G}_h(t)$. A direct least-squares fitting to it gives $\beta=0.338\pm0.003$, in excellent agreement with results from the width.

The roughness exponent χ is obtained by applying Eq. (9) to $G_h(r,t)$ in the $r\ll t^{1/z}$ regime. For a quick check, we simply used $G_h(r,t)$ at $t=1000$. We define

$$\tilde{G}_h(r,t)\equiv G_h(2r,t)-G_h(r,t) \tag{11}$$

to eliminate any additive constants. Figure 5 shows $\tilde{G}_h(r,t$

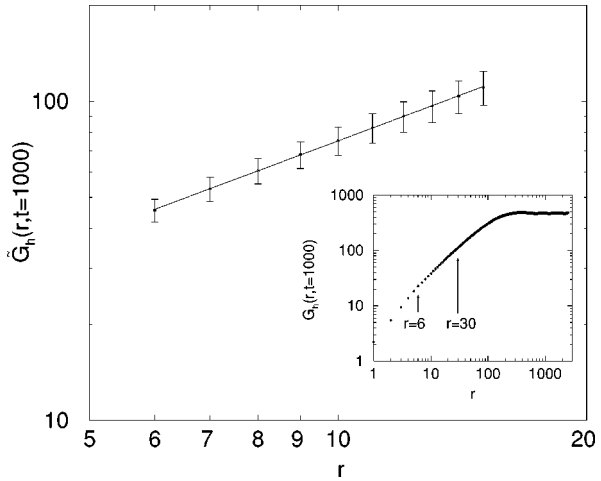

FIG. 5. $\tilde{G}_h(r,t)$ as defined in Eq. (11) applied to the curve corresponding to $t=1000$ (shown in the inset). The data points used are in the interval $r\in[6,30]$ (the scaling regime actually extends up to $r\approx100$). The slope of $\tilde{G}_h(r,t=1000)$ in this interval gives $\chi=0.49\pm0.02$.

$=1000$) on a log-log scale whose slope gives $\chi=0.49 \pm 0.02$.

Both independent estimates obtained above for β as well as the estimate for χ indicate unequivocally that the 1D fiber deposition model belongs to the KPZ universality class. The key factor determining this is the flexibility parameter T_f. In the limit where $T_f \to \infty$, the mass units comprising the fibers become unconnected at deposition and the model is equivalent to the RD. For $T_f < \infty$, however, the finite rigidity of the fibers leads to nontrivial correlations that manifest themselves as bulk defects (pores) in analogy to some other surface deposition models [2,10].

Finally, we would like to note that the crossover time t_c from RD to the KPZ regime can be estimated as follows. Since each deposition event simultaneously fills L_f sites, the width in the RD regime is

$$w_{\mathrm{RD}}(t) \approx (t/L_f)^{1/2}. \tag{12}$$

In the RD regime, the surface has no spatial correlations and hence w_{RD} is a measure also of the nearest-neighbor height differences. The RD regime ends when these become of the order T_f, such that the finite flexibility of the fibers is ''felt.'' Setting $w_{\mathrm{RD}}(t_c) \approx T_f$, we conclude that

$$t_c \approx T_f^2 L_f. \tag{13}$$

Note in particular that for any nonzero flexibility an extended RD regime appears for sufficiently long fibers $L_f \gg 1/T_f^2$. Next we shall present detailed results for the influence of T_f on growth rate and network density.

B. Growth on tilted surfaces

The average growth velocity in the vertical direction

$$v \equiv \left\langle \frac{\overline{\delta h}}{\delta t} \right\rangle \tag{14}$$

depends according to the KPZ equation (1) on the local surface slopes $|\nabla h|$. Taking an average it can be written as

$$v = v_0 + \frac{\lambda}{2} \langle \overline{(\nabla h)^2} \rangle, \tag{15}$$

where the slopes are assumed to be small. By introducing an overall tilt $m \equiv \nabla h$ to the network the velocity can be written as

$$v(m) = v(0) + \frac{\lambda}{2} m^2. \tag{16}$$

Thus, by measuring v as a function of m we can get an estimate for λ. Through the relation $v(m) = 1/\rho(m)$ this also provides information on the deposit density ρ [10].

Figure 6 shows the typical behavior of $v(m)$ for both small and large values of m. It demonstrates that $v(m)$ has two regions. For small values of m, it follows Eq. (16), as shown by the dashed line, while for large values of m the dependence becomes linear. We can define the crossover tilt m_c between these two regions by the point of intersection of Eq. (16) and the linear fit, as shown in the figure. In Fig. 7

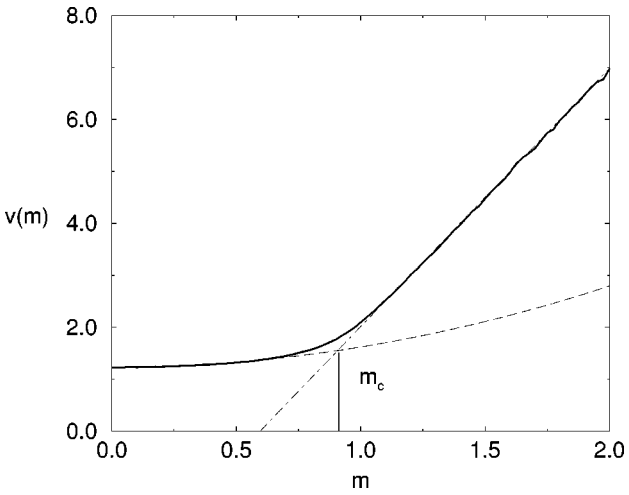

FIG. 6. Typical data for $v(m)$ (solid line) as a function of the tilt m of the substrate as $L=2500$, $T_f=1.0$, and $L_f=11$. The dashed line is a fit of the form of Eq. (16) and the dot-dashed line is calculated from Eq. (19). Their intersection defines m_c.

we plot m_c as a function of the fiber flexibility T_f for four different fiber lengths L_f. The plot shows that

$$m_c \approx T_f. \tag{17}$$

In the following we study the two limits of $v(m)$ separately and develop analytic arguments to explain its behavior.

1. Large tilts

The linear regime for the growth velocity as a function of tilt evident in Fig. 6 is easy to obtain with the following arguments. Upon deposition, the fibers tend to conform along the surface according to the amount given by the stiffness parameter T_f. However, for increasing m with $T_f < m$, each deposited fiber on the average touches the network only with one of its ends and the rest of the fiber hangs in midair. This situation is analogous to the case of *columnar growth*

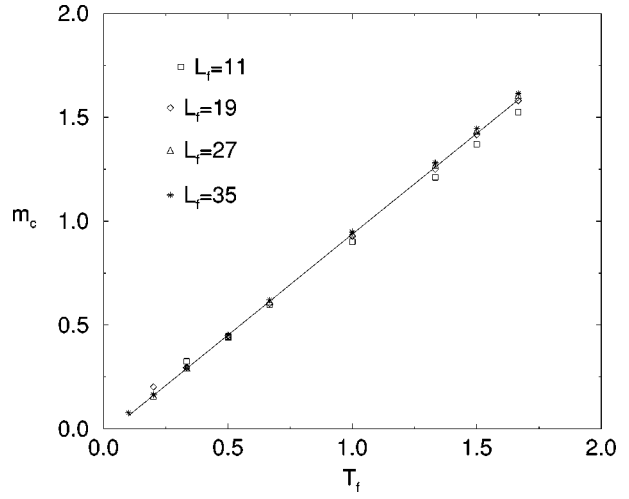

FIG. 7. Quantity m_c as a function of T_f for four different values of L_f. The number of layers deposited in each simulation was 500 and the number of runs was 10. The solid line is a numerical fit of the form $m_c = 0.97 T_f - 0.03$.

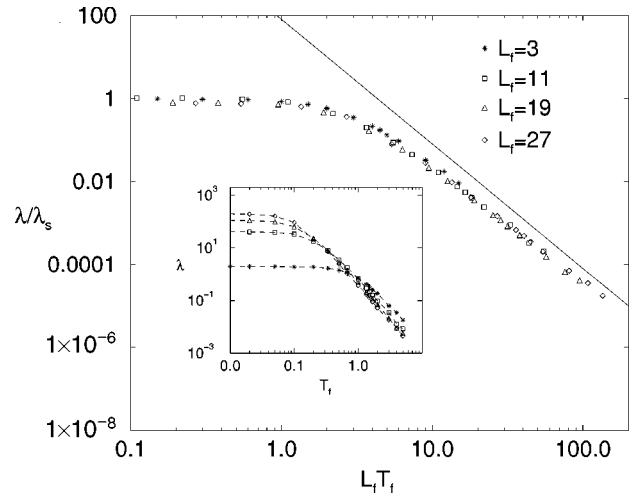

FIG. 8. Ratio λ/λ_s as a function of $L_f T_f$. This curve was obtained by collapsing four $\lambda(T_f)$ curves corresponding to $L_f=3$, 11, 19, and 27 (shown in the inset) into a single curve. In the simulations the number of layers deposited was 500 and the number of runs was 10. The solid line obeys $\lambda/\lambda_s \sim (L_f T_f)^{-3}$.

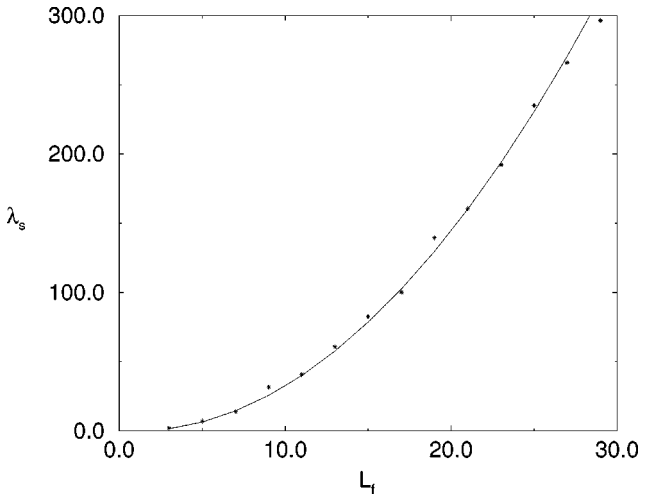

FIG. 9. Parameter λ_s as a function of L_f. The solid line shows the curve $\lambda_s = c(L_f-1)^2$ with $c=0.40$.

observed in some deposition models at oblique incidence [18]. The area between the fiber and the network (with the area of the fiber included) is

$$A = L_f + \sum_{i=1}^{L_f-1} i(m-T_f)$$

$$= L_f + \frac{1}{2}L_f(L_f-1)(m-T_f). \tag{18}$$

The average increase in the surface height per unit time is $(A/L)(L/L_f)$. The growth velocity of the system can then be written as

$$v(m) = \frac{A}{L}\frac{L}{L_f} + v_\infty$$

$$= \frac{1}{2}(L_f-1)(m-T_f)+2, \quad m > T_f, \tag{19}$$

where $v_\infty \equiv v(T_f=\infty)=1$ in our units. The validity of Eq. (19) was verified quantitatively for a system with $L=2500$, $T_f=1.0$, and $L_f=11$ for which it gives $v(m)=5.0m-3.0$ as $m>1.0$. This equation is indicated in Fig. 6 as a dot-dashed line and it shows perfect agreement with the data.

2. Small tilts

For small tilts and with $m \ll T_f$, the growth rate $v(m)$ is of the form of Eq. (16). The nonlinearity parameter λ can be then determined by least-squares fitting. Figure 8 shows how λ depends on the fiber flexibility T_f for four fiber lengths L_f when the system size is $L=2500$. The original data (shown in the inset) collapse into a single scaling curve by multiplying T_f by L_f and dividing λ by $\lambda_s \equiv \lambda(T_f=0)$ corresponding to a stiff fiber.

In the stiff fiber limit, λ_s was calculated separately as a function of L_f and the result is shown in Fig. 9. The least-squares fitting method suggests for it the quadratic function

$$\lambda_s = c(L_f-1)^2, \tag{20}$$

where $c=0.40\pm0.03$.

According to Fig. 8, in the case of small tilts λ has two regimes roughly separated by $L_f T_f \approx 1$. As $L_f T_f \ll 1$, $\lambda \approx \lambda_s$ and it does not depend on T_f. On the other hand, in the $L_f T_f \gg 1$ regime there is clearly an inverse power law behavior as a function of T_f. When the running exponent method was applied to λ/λ_s corresponding to the case of $L_f=27$, it gave for the value of the exponent of this power law -2.8 ± 0.4, implying that $\lambda/\lambda_s \sim (L_f T_f)^{-2.8}$. Thus we can summarize the scaling behavior of λ as

$$\lambda \sim \begin{cases} (L_f-1)^2 & \text{for } L_f T_f \ll 1 \\ L_f^{-1} T_f^{-2.8\pm0.4} & \text{for } L_f T_f \gg 1. \end{cases} \tag{21}$$

We note that this form correctly satisfies the RD limits of the model where $\lambda \to 0$ for either $L_f=1$ or $T_f \to \infty$.

To explain Eq. (21) we develop a simple scaling theory. In addition to the fiber length L_f, the two characteristic slopes T_f and m define the horizontal scales a/m and a/T_f, where $a=1$ is the vertical lattice constant (the thickness of the fibers). For $L_f \gg 1$, which corresponds to the physically interesting situation, the lattice length scale may be ignored and we can assume that the macroscopic features of the model depend only on the dimensionless numbers $L_f T_f$ and $L_f m$. Thus we can write

$$v(m) = \Phi(L_f m, L_f T_f). \tag{22}$$

If Eq. (22) is a smooth function of m, we obtain by the Taylor series expansion in the neighborhood of $m=0$,

$$v(m) \approx v_0(L_f T_f)[1 + \tfrac{1}{2}C(L_f T_f)L_f^2 m^2], \tag{23}$$

where

$$C = \Phi(0,\beta)^{-1}\frac{\partial^2}{\partial \alpha^2}\Phi(\alpha,\beta) \tag{24}$$

at $\alpha = L_f m = 0$ and $\beta = L_f T_f$. Thus, from Eq. (23),

$$\lambda = L_f^2 C(L_f T_f). \tag{25}$$

For $T_f \to 0$ one obtains the case of stiff fibers, which have a nonzero λ. Hence the scaling function C in Eq. (24) becomes a constant and

$$\lambda \sim L_f^2 \quad \text{for} \quad L_f T_f \ll 1. \tag{26}$$

For $L_f \gg 1$ this is in agreement with Eq. (21).

To explain the other scaling limit of λ, we consider the surface width which for the KPZ equation obeys [19]

$$w_{\mathrm{KPZ}}(t) \approx (K^2 \lambda t)^{1/3} \tag{27}$$

in the asymptotic time-dependent growth regime. The constant K is defined through the stationary height difference correlation function [cf. Eq. (8)]

$$\lim_{t \to \infty} G_h(r,t) \approx K|r|. \tag{28}$$

Since the stationary interface is essentially a random walk along h, K can be interpreted as the square of the typical height difference between subsequent sites. Thus, for large T_f [20]

$$K \approx T_f^2. \tag{29}$$

We now estimate the crossover time t_c from the RD to the KPZ regime by equating Eqs. (12) and (27), which yields, using Eqs. (25) and (29),

$$t_c \approx L_f^3 (K^2 \lambda)^2 \sim L_f^7 T_f^8 C^2 (L_f T_f). \tag{30}$$

Comparing this to the previously derived expression (13) gives

$$C(L_f T_f) \sim (L_f T_f)^{-3}, \tag{31}$$

which, when substituted into Eq. (25), leads to

$$\lambda \sim \frac{1}{L_f T_f^3}, \quad L_f T_f \gg 1. \tag{32}$$

This agrees reasonably well with the numerical result in Eq. (21). The solid line in Fig. 8 shows $\lambda/\lambda_s \sim (L_f T_f)^{-3}$. To lend support to the validity of Eq. (32), in the Appendix we present another argument that gives the same result based on purely geometric considerations.

IV. SUMMARY AND CONCLUSIONS

In this work we have studied the kinetic roughening of surfaces of random fiber deposits in one dimension through a simple model. In the model, fibers of length L_f are randomly deposited on a lattice and allowed to bend down upon touching the deposit by an amount determined by the flexibility T_f. For any finite value of T_f, following an initial random deposition regime, a nontrivial pore structure develops in the bulk and the consequent kinetic roughening of the growing surface is characterized by the KPZ universality class. We have also studied in detail the dependence of the nonlinear coefficient λ on the parameters of the model and developed analytic arguments to explain the tilt dependence of the growth velocity v. Results from numerical simulations are in good agreement with these arguments.

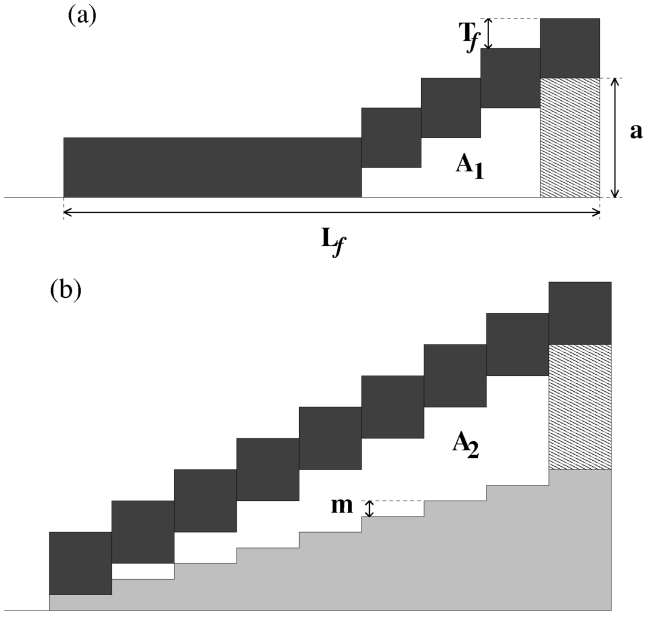

FIG. 10. Geometric argument for Eq. (32). See the text for details.

The results of this paper point out the possibility of studying kinetic roughening in the deposition of fiberlike or platelike objects, similarly to Ref. [16]. Although we have not discussed the 2D version of the deposition model here, many of the conclusions presented for the 1D case can be extended to higher dimensions as well. In particular, due to the tilt dependence of growth inherent in the model, the kinetic roughening should be described by the KPZ equation.

ACKNOWLEDGMENTS

This work was in part supported by the Academy of Finland through the MATRA program. J.K. acknowledges the kind hospitality of HIP during a visit when this work was initiated and support by the DFG under Grant No. SFB 237 (Unordnung und Grosse Fluktuationen).

APPENDIX: GEOMETRIC ARGUMENT FOR λ AT SMALL TILTS

We have developed another argument to support the validity of the inverse power law of Eq. (32) by using geometric reasoning similar to what was applied successfully in the large tilt regime. Consider a fiber lying on a horizontal substrate in such a way that its left end is supported by a column of height a [see Fig. 10(a)]. The fiber is sufficiently long so that the right end touches the substrate. The empty space between the substrate and the fiber has an area of

$$A_1 = \sum_{i=1}^{a/T_f} (a - iT_f) = \frac{a^2 - aT_f}{2T_f}. \tag{A1}$$

Next the substrate is tilted by m so that both ends of the fiber still have something to touch beneath them [Fig. 10(b)]. The condition for this is

$$\frac{a}{T_f-m}<L_f-1. \tag{A2}$$

The area of the empty space between the fiber and the substrate is now

$$A_2=\sum_{i=1}^{a/(T_f-m)}[a+i(m-T_f)]=\frac{a^2+am-aT_f}{2(T_f-m)}. \tag{A3}$$

Thus the tilting introduces a change of

$$\Delta A_l\equiv A_2-A_1=\frac{a^2+am-aT_f}{2(T_f-m)}-\frac{a^2-aT_f}{2T_f}$$

in the area. By using the Taylor expansion for $m\ll 1$ we obtain

$$\Delta A_l\approx\frac{a^2}{2T_f^2}m+\frac{a^2}{2T_f^3}m^2. \tag{A4}$$

A reversal of the fiber is clearly equivalent to reversing the sign of the tilt. The change in area for a fiber supported at its right end is therefore

$$\Delta A_r\approx-\frac{a^2}{2T_f^2}m+\frac{a^2}{2T_f^3}m^2. \tag{A5}$$

By symmetry, the number of fibers of the two types is the same for an untilted substrate. The contributions to Eqs. (A4) and (A5) that are linear in m therefore cancel and the net change in area is

$$\Delta A\sim\Delta A_l+\Delta A_r\sim\frac{1}{T_f^3}m^2. \tag{A6}$$

The corresponding change in growth rate is then

$$v(m)=\frac{\Delta A}{L}\frac{L}{L_f}\sim\frac{1}{L_fT_f^3}m^2 \tag{A7}$$

which by Eq. (16) leads to Eq. (32).

[1] A.-L. Barabási and H. E. Stanley, *Fractal Concepts in Surface Growth* (Cambridge University Press, Cambridge, 1995).

[2] J. Krug, Adv. Phys. **46**, 139 (1997).

[3] M. Kardar, G. Parisi, and Y. C. Zhang, Phys. Rev. Lett. **56**, 889 (1986).

[4] F. Family and T. Vicsek, J. Phys. A **18**, L57 (1985).

[5] J. Maunuksela, M. Myllys, O.-P. Kähkönen, J. Timonen, N. Provatas, M. J. Alava, and T. Ala-Nissila, Phys. Rev. Lett. **79**, 1515 (1997).

[6] K. J. Niskanen and M. J. Alava, Phys. Rev. Lett. **73**, 3475 (1994).

[7] E. K. O. Hellén, M. J. Alava, and K. J. Niskanen, J. Appl. Phys. **81**, 6425 (1997).

[8] A. Koponen *et al.*, Phys. Rev. Lett. **80**, 716 (1998).

[9] K. Niskanen, N. Nilsen, E. Hellén, and M. Alava, in *Proceedings of the 11th Fundamental Research Symposium (Cambridge, UK, 1997)*, edited by C. F. Baker (Pira International, in press), p. 1273.

[10] M. Schimschak, and J. Krug, Phys. Rev. B **52**, 8550 (1995).

[11] E. Seppälä, M. Alava, and K. Niskanen, Paperi ja Puu **78**, 446 (1996).

[12] N. Provatas, M. J. Alava, and T. Ala-Nissila, Phys. Rev. E **54**, R36 (1996).

[13] N. Provatas, M. Haataja, E. Seppälä, S. Majaniemi, J. Åström, M. Alava, and T. Ala-Nissila, J. Stat. Phys. **87**, 385 (1997).

[14] S. Schwarzer, Phys. Rev. E **52**, 6461 (1995).

[15] M. L. Kurnaz and J. V. Maher, Phys. Rev. E **53**, 978 (1996); K. V. McCloud, M. L. Kurnaz, and J. V. Maher, *ibid.* **56**, 5768 (1997).

[16] J. D. Sherwood and H. Van Damme, Phys. Rev. E **50**, 3834 (1994).

[17] T. Ala-Nissila, T. Hjelt, J. M. Kosterlitz, and O. Venäläinen, J. Stat. Phys. **72**, 207 (1993).

[18] J. Krug and P. Meakin, Phys. Rev. A **40**, 2064 (1989); **43**, 900 (1991).

[19] J. Krug, P. Meakin, and T. Halpin-Healy, Phys. Rev. A **45**, 638 (1992).

[20] For stiff fibers with $T_f=0$, it is clear from dimensional considerations that $K\approx 1/L_f$. We therefore expect a crossover from $K\approx T_f^2$ to $K\approx 1/L_f$ at $T_f\approx 1/\sqrt{L_f}$.